Tacticity Effects on Polymer Blend Miscibility. 1. Flory–Huggins–Staverman Analysis[†]

G. Beaucage[*,‡] **and R. S. Stein**

Department of Polymer Science and Engineering, University of Massachusetts, Amherst, Massachusetts 01003

R. Koningsveld

Polymer Institute Σ Π, Waldfeuchstraat 13, 6132 HH Sittard, The Netherlands

Received May 5, 1992; Revised Manuscript Received November 5, 1992

ABSTRACT: In a previous paper isotactic poly(vinyl methyl ether) (PVME), synthesized in our laboratory, and heterotactic PVME were characterized by GPC, NMR, X-ray diffraction, and DSC. Cloud-point measurements were used to demonstrate that isotactic PVME is less miscible with atactic PS than heterotactic PVME. In this paper Flory–Huggins–Staverman (F–H–S) theory is used to relate shifts in miscibility to changes in the entropic component of the composition-dependent interaction parameter, "*g*", and to changes in the Staverman parameter, "*c*". In the F–H–S approach a composition-dependent interaction parameter is explicitly related to the relative surface areas for lattice sites of the two components. The relative surface area can be determined from low molecular weight materials using the method of Bondi, from simple molecular models, and from a fit to the cloud-point curve. For tactic blends these methods are compared. A distinct difference in the relative surface area for isotactic and atactic PVME is observed which can partially account for shifts in miscibility. A fractionation effect is predicted for polydisperse blends. Uniquely at the critical point fractionation of polydisperse components is not observed.

Introduction

In a previous paper[1] we reported reduced miscibility for isotactic PVME in comparison to atactic (predominantly heterotactic) PVME when blended with atactic PS. Shifts in miscibility were related to changes in the eutropic component of the composition-dependent χ-parameter "*g*" using classic Flory–Huggins theory. In this paper we further analyze two cloud-point curves using Flory–Huggins–Staverman theory.[2,3] An expression is derived which accounts for the composition and temperature dependence of *g* for the isotactic and atactic PVME in blends with PS.

Theoretical Background

Phase separation in the polystyrene/poly(vinyl methyl ether) (PS/PVME) blend system exhibits LCST behavior and can be conveniently studied using light scattering due to the large difference in the index of refraction between PVME and PS (1.467 and 1.592, respectively). By slowly raising the temperature of a polymer blend of composition ϕ (where ϕ is the PVME volume fraction), the optical cloud point (T_{CP}) can be determined. The cloud-point curve (CPC) determined by extrapolating T_{CP} versus ϕ_2 data to zero heating rate can be related to the binodal phase diagram (the locus of coexisting phase compositions in $T{:}\phi_2$ space) for monodisperse polymer blends. It is not permitted to identify the cloud-point curve (CPC) with the binodal for polydisperse blends. The polystyrene samples studied here have a narrow molecular weight distribution which is represented by a single component in this analysis. The distribution of the PVME samples, however, is rather broad and cannot be ignored. The significance of a two-dimensional phase diagram (temperature versus composition) for a nonbinary system has been amply discussed;[2-8] here the situation is summarized in Figure 1 which shows that cloud points coexist with

Binary Composition →
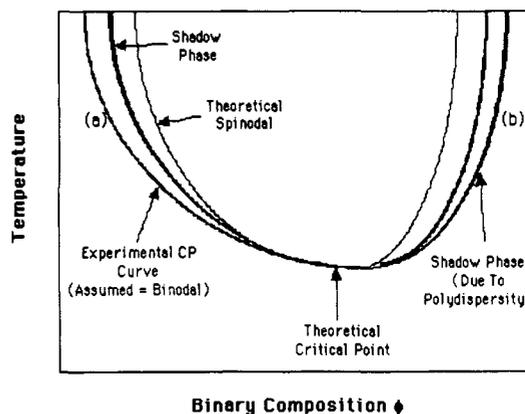
Figure 1. Theoretical and experimental CP curves (one of the components is polydisperse).

incipient phases (shadow phase) whose overall concentration differs from those lying on the CPC (the tie line phase) except at the critical point. The polymer fractions in the incipient phases (coexisting phases), connected by the shadow curve (SHP), also differ from the original polymer in molecular weight distribution (i.e., a fractionation of molecular weight occurs on phase separation for polydisperse blends). Thus, a blend at the cloud point (a) on the left side of Figure 1 is in equilibrium with the shadow phase (b) on the right side, and the molecular weight of the shadow phase differs from that of the parent, cloud-point phase.

Flory–Huggins–Staverman Approach

Modeling the systems as quasi-binary mixtures in which constituent 1, polystyrene, is monodisperse and constituent 2, PVME, contains a distribution of chain lengths, we have, at two-phase equilibrium,

$$\Delta\mu_1^a = \Delta\mu_1^b \tag{1}$$

$$\Delta\mu_{2i}^a = \Delta\mu_{2i}^b \tag{2}$$

In these equations $\Delta\mu_k^1$ is the chemical potential of component k in phase 1 minus the value for the pure component k in the liquid state at the same pressure and temperature. There are as many equations as there are components in constituents 1 and 2.

To find expressions for the $\Delta\mu$'s, we assume the system to obey the Flory–Huggins rigid lattice equation for the free enthalpy of mixing ΔG amended for the difference in size between styrene and vinyl methyl ether units (Flory–Huggins–Staverman approach[2-8]),

$$\frac{\Delta G}{NRT} = \frac{\phi_1}{m_1} \ln \phi_1 + \sum\left(\frac{\phi_{2i}}{m_{2i}} \ln \phi_{2i}\right) + g\phi_1\phi_2 \quad (3)$$

where ϕ_1 and ϕ_2 are the volume fractions of PS and PVME, respectively, m_j is the number of lattice sites occupied by macromolecules "j", N is the total number of lattice sites in moles, and RT has its usual meaning. We have

$$\phi_2 = \sum \phi_{2i} \quad (4)$$

and define the interaction function g (we use g for a composition-dependent χ parameter) by

$$g = a + \frac{(b_0 + b_1/T)}{(1 - c\phi_2)} \quad (5)$$

where a and b_0 are parameters correcting for possible shortcomings in the first two combinatorial entropy terms on the right-hand side of eq 3. The parameter b_1 is of an enthalpic nature,

$$\frac{b_1}{T} = \frac{z_2 \Delta w_{12}}{RT} \quad (6)$$

and

$$c = 1 - \frac{z_2}{z_1} \approx 1 - \frac{s_2}{s_1} \quad (7)$$

c will here be referred to as the Staverman parameter. The coordination numbers z_2 and z_1 refer to the two repeat units in the system and are supposed to reflect their difference in size and shape. We follow Staverman in further assuming the ratio z_2/z_1 equals the ratio of molecular surface areas s_2/s_1 (see ref 2) which can be estimated with Bondi's method of group contributions.[9] Alternatively, c can be used as an adaptable parameter.

It should be noted that the Flory–Huggins (F–H) lattice model assumes equally sized and symmetrically shaped lattice sites such as would exist in a polymer/symmetric solvent system where the size of the solvent molecule defines the lattice cell size. For real polymer/polymer systems a symmetric lattice cell with one mer unit per cell is probably not the case. Regardless of the real situation, the statistics involved in deriving the F–H theory as originally formulated do not allow for deviation from a strictly symmetric and generally small sized lattice site. Thus, the present discussion must be taken as indications of where newer theories for polymer blends (such as the Curro–Schweitzer PRISM theory[10]) should be directed and as a qualitative indication of the results to be expected from such modern theories. (The PRISM theory is not at this date capable of describing the phenomena involved in this paper but does account for surface area differences similar to those described by the Staverman parameter.)

If $z_2 = z_1$, the interaction function, g, is independent of concentration and is usually denoted by χ. We note that the entropic and enthalpic contributions to χ, χ_s, and χ_h,

respectively, are then given by

$$\chi_s = a + b_0 \quad (8)$$

and

$$\chi_h = b_1/T \quad (9)$$

It has been demonstrated that the parameters a and b_0 are not merely empirical in nature. They can be shown to arise from combinatorial entropy corrections due to a disparity between z_1 and z_2.[2] In the present work we use a and b_0 as adaptable parameters.

Within this framework the chemical potential of the components are given by (see, for example, ref 11)

$$\frac{\Delta\mu_1}{m_1 RT} = \frac{\ln \phi_1}{m_1} + \left(\frac{1}{m_1} - \frac{1}{m_{n2}}\right)\phi_2 + g_1\phi_2^2 \quad (10)$$

$$\frac{\Delta\mu_{2i}}{m_{2i}RT} = \frac{\ln \phi_{2i}}{m_{2i}} + \frac{1}{m_{2i}} - \frac{1}{m_1} + \left(\frac{1}{m_1} - \frac{1}{m_{n2}}\right)\phi_2 + g_2\phi_1^2 \quad (11)$$

where

$$g_1 = a + \frac{b(1 - c)}{(1 - c\phi_2)^2} = g - \phi_1\left(\frac{\delta g}{d\phi_2}\right) \quad (12)$$

$$g_2 = a + \frac{b}{(1 - c\phi_2)^2} = g - \phi_2\left(\frac{\delta g}{d\phi_1}\right) \quad (13)$$

$$b = (b_0 + b_1/T) \quad (14)$$

and

$$m_{n2} = \sum \frac{\phi_2}{\phi_{2i}/m_{2i}} \quad (15)$$

Polydispersity

Dealing with eqs 1, 2, 10, and 11, we are faced with the problem of the molecular weight distribution in constituent 2. Three average molecular weight values are available, viz., number-, weight-, and Z-average, M_N, M_W, and M_Z. The following definitions may be formulated:

$$\sum w_i = 1 \quad (16)$$

$$\sum \frac{w_i}{M_i} = \frac{1}{M_N} \quad (17)$$

$$\sum w_i M_i = M_W \quad (18)$$

$$\sum w_i M_i^2 = M_W M_Z \quad (19)$$

where the w_i represent the mass fraction of component "i" with molecular weight M_i, the total mass being normalized to 1 g.

Since there are only four equations, the molecular weight distribution (w_i, M_i) can be established in a unique fashion only for a binary polymer mixture, where we have four unknowns $(w_1, w_2, M_1$ and $M_2)$ representing the distributions of the PVME samples.

Determination of the Parameters a, b_0, and b_1

The principal effect of the introduction of a molecular weight distribution is a shift of the critical solution point away from the minimum in the CPC. The CPC and its coexistence curve (SHP) are determined by eqs 10 and 11, the use of which calls for knowledge of the parameters a,
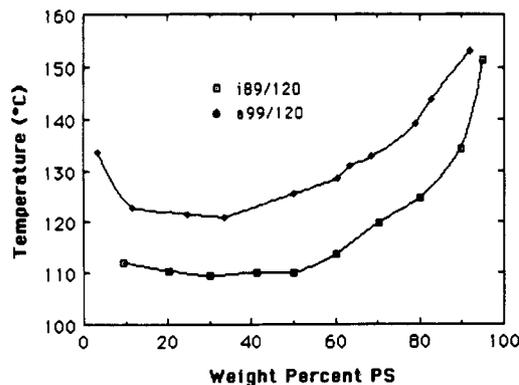
Figure 2. Cloud-point curves for i89/120 and a99/120 blends (lines merely connect the data points).

b, and *c*. If the molecular weight distribution in constituent 2 were completely known, one might represent it either by an arbitrary number of components or by a continuous function and fit the data to eqs 10 and 11. Alternatively, one might use the spinodal and critical conditions given respectively by

$$\frac{1}{m_{W1}\phi_1} + \frac{1}{m_{W2}\phi_2} = 2a + \frac{2b(1-c)}{(1-c\phi_2)^3} \qquad (20)$$

$$\frac{\alpha_1}{m_{W1}\phi_1^2} + \frac{\alpha_2}{m_{W2}\phi_2^2} = \frac{6bc(1-c)}{(1-c\phi_2)^4} \qquad (21)$$

where m_{Wj} is the weight-average site number of constituent "*j*" and $\alpha_j = (M_Z/M_W)_j$.

Experimental Section

Isotactic PVME, i89 (M_W = 89 000, M_N = 49 100, M_Z = 144 900), was prepared using cationic polymerization followed by solvent fractionation as previously reported.[1] Atactic PVME, a99 (M_W = 99 000, M_N = 46 500, M_Z = 151 300), was purchased from Scientific Polymer Products Inc. and fractionated.[1] The triad tacticities of the two polymers were determined using proton NMR (a99, 31% isotactic and 69% heterotactic; i89, 55% isotactic, 40% heterotactic, and 5% syndiotactic). The glass transition temperature for the two polymers was essentially identical, -29 °C, in accord with the findings of Karasz and MacKnight[12] for other monosubstituted vinyl polymers. Relatively monodisperse PS, M_w/M_n = 1.03, of molecular weight M_w = 120 000 (Polymer Laboratories, Amherst, MA) was blended with each of the two PVME samples. Molecular weights of all polymers are reported as measured by GPC in terms of polystyrene standards. A Mark–Houwink analysis of the isotactic and heterotactic PVME indicated that this led to errors in the molecular weight of less than 5% which is within the accuracy of the measured values.

Blends of PVME/PS were cast from toluene solutions at 30 °C and allowed to air dry. The films were further dried in a vacuum oven at 70 °C for a week and finally in a vacuum oven at 100 °C for at least 6 h before scattering measurements were made. Cloud-point measurements were performed on relatively thick films, 50–100 μm, cast on one microscope cover slip. Integrated scattering intensity from an angular range of about 50 to 140° was measured using an apparatus previously described.[1] Samples for the cloud-point measurements were equilibrated in the hot stage at temperatures close to the phase-separation temperature prior to measurements. Measurements at several heating rates were taken, and the phase-separation temperature was extrapolated to zero heating rate.

F–H–S Cloud-Point Analysis

Figure 2 is the cloud-point curve (CPC) for the i89/120 and a99/120 blends.
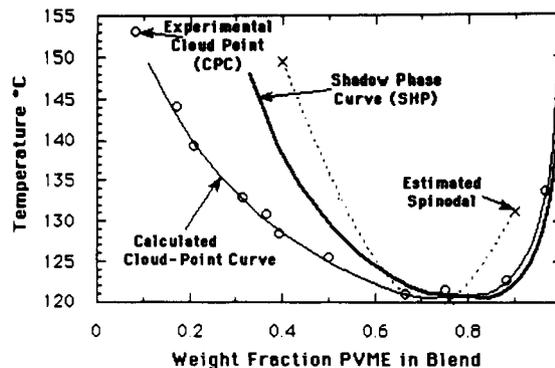
Figure 3. Flory–Huggins–Staverman fit to the CPC of the 99 000 atactic PVME/120 000 PS blend (a99/120).

Table I
Flory–Huggins–Staverman Analysis Parameters from Fits to the Cloud-Point Curves

	a (×10³)	b_0 (×10²)	b_1	c
atactic	-1.43	1.36	-4.69	0.36[a]
isotactic	-0.57	1.77	-4.08	0.425
Δvalue	0.86	0.20	0.14	0.17
avg value				

[a] From Bondi.[9]

Both blends contain the same molecular weight PS but different M_W for the two PVME's. In spite of the fact that the molecular weight of the PVME in a99/120 is higher than that for i89/120, the cloud-point curve for a99/120 is higher than that for i89/120, implying a tacticity effect. Thus the isotactic PVME is less miscible with PS than the atactic PVME. Figure 3 shows the Flory–Huggins–Staverman fit to the CPC of the 99 000 atactic PVME/120 000 PS blend (a99/120). Polydispersity significantly shifts the composition of the coexisting incipient phase (SHP) from the cloud-point curve.

Polydispersity of the PVME component was accounted for by representing the polydisperse polymers as a mixture of two monodisperse polymers. The procedure involved calculating two monodisperse PVME fractions, M_1 = 26 900, w_1 = 0.499 and M_2 = 170,800, w_2 = 0.501, from the molecular weight distributions and eqs 16–19 (given the three molecular weight distributions, a unique solution for M_1, w_1, M_2, and w_2 is possible). Next, three spinodal points were estimated such that the central spinodal point would approximate T_{CP} for a 0.75 weight fraction PVME blend. Equations 20 and 21 were then used to calculate a, b_0, and b_1 using c = 0.36 as calculated from Bondi.[4] These values for a, b_0, and b_1 were then used in equations 1, 2, and 10–15 to generate the binodal and shadow curves. This procedure was iterated, varying the off-critical spinodal points ("×" in Figures 3 and 4), until an optimal fit to the CPC was obtained. The final values for a, b_0, and b_1 are reported in Table I. (It should be noted that the monodisperse molecular weight fractions do not necessarily have values close to 0.5. For the isotactic PVME M_1 = 34 100, w_1 = 0.623 and M_2 = 179 600, w_2 = 0.377.)

Figure 4 is a similar fit to the i89/120 blend. Since the surface area of the isotactic polymer may differ from that of the atactic polymer, the Bondi value for the Staverman parameter, "*c*", was not used for the isotactic PVME/PS blend. For the isotactic blend use was made of the inherent relationship between b_1 and c derived from eqs 6 and 7 (the definition of *c*). (This technique was called the "Bondi-constraint" method by Beckman et al.[3]) If it is assumed that the coordination number z_1 or the surface area s_1 for the PS component is the same for both the
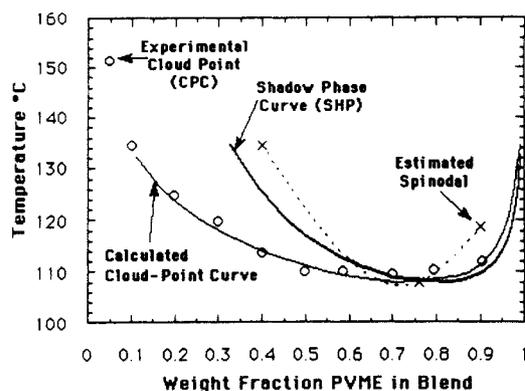
Figure 4. Flory–Huggins–Staverman fit to the CPC of the i89/120 blend.

isotactic and atactic blends, then

$$\frac{b_{1i}}{b_{1a}} = \frac{(1 - c_i)}{(1 - c_a)} \tag{22}$$

Thus, using the Bondi value for c_a (the atactic Staverman parameter), one may obtain a value for c_i, a_i, b_{0i}, and b_{1i} (the isotactic values), using the same iterative scheme. In this way a value for c_i of 0.425 was obtained, indicating a smaller PVME surface area for the isotactic blend in relation to the atactic blend. It should be noticed that the fit to the CPC at high and low concentrations is strongly affected by c, such that if one were to use the Bondi value of 0.36 for the isotactic blend, a noticeable mismatch with the CPC would occur.

Values for a, b_0, b_1, and c for the isotactic and atactic blends are presented in Table I. The fractional change relative to an average value is also reported. The tacticity difference most strongly affects the entropic terms a and b_0 as well as the Staverman parameter, c. Since g is related to $\Delta G/T$ and $\Delta G/T = \Delta H/T - \Delta S$, the change in the entropic terms is related to a negative change in the entropy. That is to say, in comparing the ground state for the blend components with their state in the blend, there is a smaller change in the non-composition-dependent entropy, "a", on mixing for the isotactic PVME than for the atactic PVME, and this change is toward a more random state for both. The composition-dependent entropy term, b_0, shows a larger change on mixing for the isotactic PVME, and this is a change toward a more ordered state. Composition is measured in terms of the weight fraction of PVME in the blend (ϕ_2). The change in the Staverman parameter, c, reflects a smaller surface area for the isotactic PVME in comparison to the atactic PVME which will be discussed with respect to simple molecular models. In considering the net effect of the parameters listed in Table I, a plot of the composition dependence of the entropic $[a + b_0/(1 - c\phi)]$ and the enthalpic $[b_1/\{T(1 - c\phi)\}]$ components of g (composition-dependent χ) will be considered (Figure 5).

Figure 5 shows a more positive value for g in the isotactic blend which leads to the tacticity effect (a more positive value for g indicates lower miscibility). The difference in the enthalpic component of g, for the isotactic and atactic PVME blends, is small compared with the entropic component. The differences in the entropic component become larger at higher fractions of PVME, while the enthalpic differences become smaller. The dominance of the entropic terms and the changes in the Staverman parameter, c, indicate that the isotactic PVME in the blend shows a higher degree of ordering (and tighter packing) than the atactic PVME in comparison to the melts for the
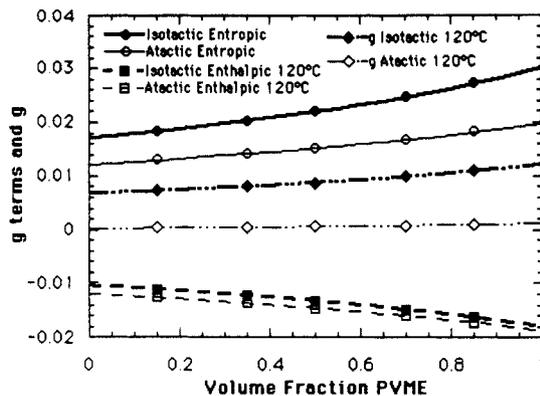
Figure 5. Entropic $[a + b_0/(1 - c\phi)]$ and enthalpic $[b_1/\{T(1 - c\phi)\}]$ components of g (composition-dependent χ) at 120 °C for the isotactic and atactic PVME/PS blends.
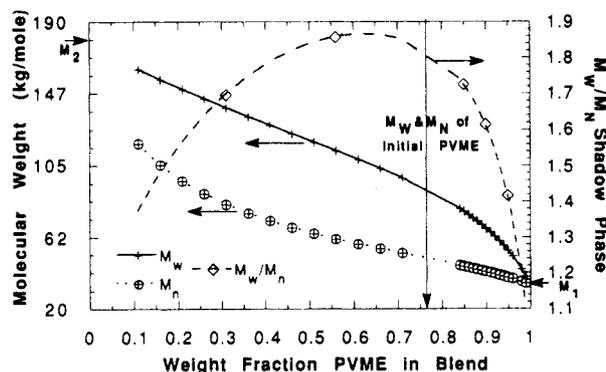
Figure 6. Fractionation of PVME in the incipient phase (coexisting phase) for the isotactic blend. M_W, M_N, and M_W/M_N of the incipient phase versus initial blend composition in weight fraction PVME (initial phase polydispersity is indicated by the arrow). M_1 and M_2 are the binary components used to model the polydisperse PVME.

two materials. This leads to a relatively large decrease in entropy (the negative of the entropic terms as discussed above). Thus one is led to the conclusion that the isotactic PVME in some way becomes more ordered in the blend; that is, interactions with PS in the blend increase the ordering of the isotactic PVME more than atactic PVME when compared with the ground-state melts. (The ability of isotactic PVME to order in minimum-energy conformations will be discussed in regard to simple molecular models.) It is noted that this purported ordering increases with the fraction PVME in the blend. Thus it is probably a property which relates to the structural nature of the PVME component, specifically the tacticity.

The dominance of the entropic term in the shift in miscibility for the isotactic PVME/PS blends agrees with the critical point analysis given in a previous publication.[1]

Fractionation in Phase-Separating Blends

The fractionation of polymers in phase separation from polydisperse blends has not been extensively described in the literature. A dramatic fractionation of the polydisperse PVME is predicted by the F–H–S theory. Figures 6 and 7 show M_W, M_N, and M_W/M_N for the shadow phase (the coexisting phase) versus the initial blend composition (cloud-point phase composition) for the isotactic and atactic PVME blends, respectively. In both blends a fractionation effect is felt at the extremes of concentration. The polydispersity goes to 1 at the extremes of composition. For a blend close to pure PVME, only the low molecular weight monodisperse fraction, M_1, is phase separated at the CPC. Similarly, for a blend close to pure PS only the high molecular weight PVME, M_2, is phase separated at
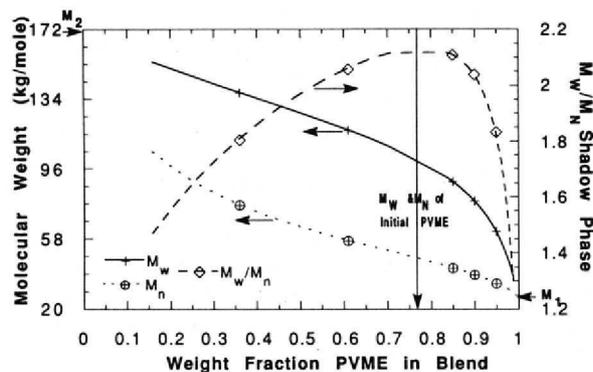
Figure 7. Fractionation of PVME in the incipient phase (coexisting phase) for the atactic blend. M_W, M_N, and M_W/M_N of the incipient phase versus initial blend composition in weight fraction PVME (initial phase polydispersity is indicated by the arrow). M_1 and M_2 are defined as in Figure 6.

the cloud point. Further, by comparing Figures 3 and 4 with Figures 6 and 7, it can be seen that only at the critical point are the original M_W and M_N of the PVME maintained (indicated by the large arrow in Figures 6 and 7). It should be noted that this fractionation effect probably has important consequences with regard to the T_g, viscosity, degree of crystallinity, and modulus of the incipient phase which is formed. In the above analysis we have only considered thermodynamic behavior which dominates at the earliest stages of phase separation. In practice the later stages of phase separation are governed by transport properties, interfacial properties of the phases being formed, and thermodynamic driving forces which would change with the composition of the phases and depth of quench. The fractionation and shifting of the incipient phase composition shown for the initial conditions should, however, serve as an indication of the general tendency for phase separation in a polydisperse blend of this type.

Estimation of $c_{PVME/PS}$ Using Simple Molecular Models

In addition to the cloud-point determination of $c_{PVME/PS}$ for the isotactic material, an estimation was made using a simple molecular modeling program[13] based on Allinger's MM2 conformational analysis technique.[14,15] Projections of the molecules were produced (shown in Figures 8–10) after performing an energy minimization for isolated isotactic and heterotactic PVME chains and heterotactic PS chains all of 20 mer units. The ordering achievable in the isotactic blends and not in the atactic blends becomes apparent after referring to Figures 8 and 9. The isotactic material is capable of forming a sheetlike structure in these simple models formed of helical chains. A heterotactic oligomer produced in the same way is shown in Figure 9. This isomer forms a completely different structure in these rudimentary models. The sheetlike form is absent. Instead, a more wormlike chain with kinks is seen. The regular structure caused by the tacticity acts to reduce the surface area of the oligomer on a scale of 6–15 mer units. Thus, it is apparent that simple models of chain interactions, such as the Hildebrand theory, which do not account for larger scale, conformational differences may be deficient.

A model for oligomeric PS of 20 mer units was also made (Figure 10). This model showed a wormlike chain with kinks as in the heterotactic PVME. A marked orientation of the aromatic side groups is observed.

From various projections of the models an estimate for the surface areas was made. These surface areas were
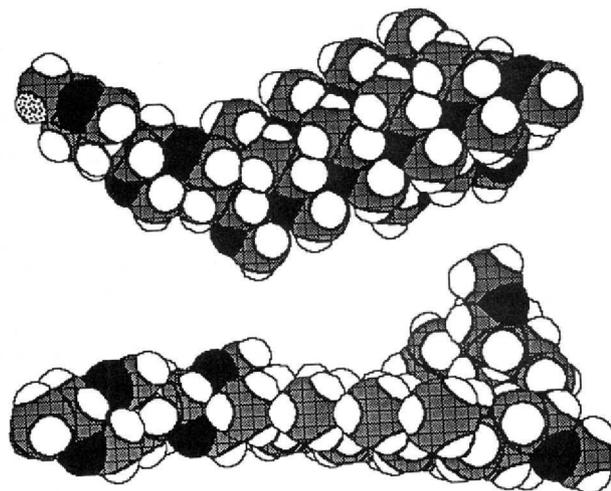
Figure 8. Isotactic PVME (two space-filling projections at 90°) with a degree of polymerization of 20. Estimated $c_{PVME/PS}$ = 0.411 (a value of 0.425 was obtained from the cloud-point fits). White regions are hydrogen, black are oxygen, and gray are carbon. The speckled hydrogen in the top view is a deuterium tag at the end of the chain.
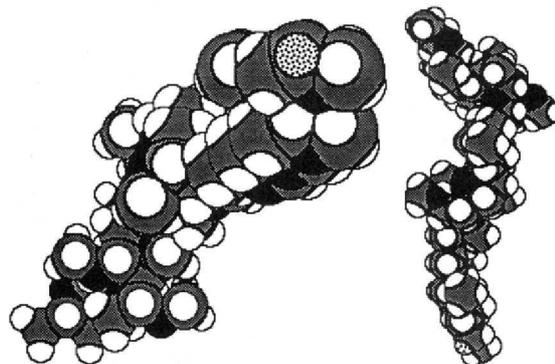
Figure 9. Heterotactic PVME with a degree of polymerization of 20. Two space-filling projections at 90° are shown, one being an end view and the other a side view. Estimated $c_{PVME/PS}$ = 0.393. A value of 0.36 was used in the cloud-point fits as determined from low molecular weight materials using the method of Bondi.
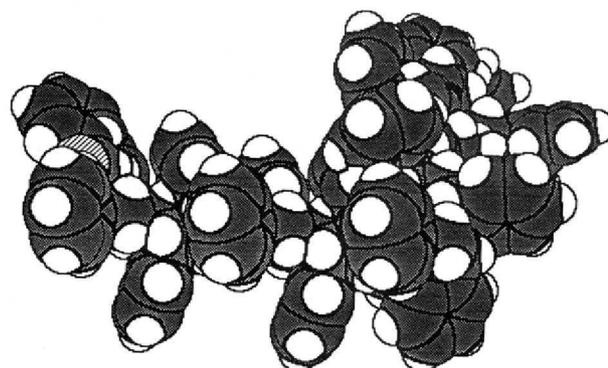
Figure 10. Heterotactic PS with a degree of polymerization of 20. This model was used to estimate the surface area of a PS chain for use in the calculation of $c_{PVME/PS}$. Gray areas are carbon, white areas hydrogen, and hatched areas deuterium-tagged end groups.

used to calculate $c_{PVME/PS}$. Values of 0.393 for the heterotactic and 0.411 for the isotactic were obtained in this way. An increase in $c_{PVME/PS}$ for the isotactic material agrees with the cloud-point measurements and the results in Table I (an increase in c was caused by a smaller surface area per mer in the isotactic oligomer). For oligomers with such a low degree of polymerization it was impossible

to mix different tacticities in the percentages observed experimentally. If this were possible, the surface area differences between isotactic and atactic PVME could be estimated more accurately. The tacticity of the PS used in the experiments was not determined but most likely contains about 25% isotactic triads. Thus the heterotactic PS surface area is probably overestimated in these models. Since $c_{PVME/PS} = 1 - S_{PVME}/S_{PS}$, this would have the effect of increasing $c_{PVME/PS}$. It should be noted that localized regions of isotactic material (Figure 8) several mer units long in a heterotactic chain (Figure 9) might serve as strong bending points in the structure, leading to a reduced available surface area such as observed experimentally and calculated using the Bondi-constraint method.

Conclusions

We have used Flory–Huggins–Staverman theory to analyze the tacticity effect for the PVME/PS polymer blend system. Generally, this analysis predicted a shift in the equilibrium phase composition in both net PVME content and in the molecular weight distribution of the phase-separated PVME from that of a conventional tie-line phase. It was predicted that, for blends of close to pure PVME, only the lowest molecular weight fraction of the PVME would phase separate into the PS-rich phase. Inversely, for blends of almost pure PS, only the highest molecular weight PVME would be separated. Uniquely, at the critical point, fractionation of the PVME did not occur on phase separation.

The parameters used in the F–H–S analysis indicated that changes in the tacticity predominantly affected the entropic component of "g". This agrees with a previous analysis based on the classic Flory–Huggins approach. Changes in the Staverman parameter, c (17%), with tacticity have been related to simple molecular models for tactic oligomers. In the second paper of this series the thermodynamic driving force for phase separation will be predicted using the parameters derived in this analysis of cloud-point curves. This driving force is indirectly related to the kinetics of phase separation in the two-phase region. Large changes in the kinetics predicted by the parameters obtained in this paper are qualitatively and quantitatively observed for tactic blends of PVME with PS. In a third paper the F–H–S parameters in the miscible regime are investigated using small-angle neutron scattering. The values obtained are compared with the cloud-point values obtained in this paper after accounting for the deuteration effect. Values of the interaction parameter in the miscible regime are revealing in terms of the mechanism involved in the tacticity effect; specifically, a relationship between

crystallization phenomena and shifts in the miscibility far above the equilibrium melting point is investigated.

The relationship between a structural view of miscibility as approximated by the F–H–S theory, and lower critical solution temperature (LCST) behavior is extensively discussed in the third paper of this series. LCST behavior is predicted from a balance between entropic factors favoring demixing and enthalpic factors favoring miscibility. In the F–H–S approach the entropic factors in g can be loosely viewed as internal structural ordering in the interacting units. It will be argued that internal ordering of the interacting units is related to the volume of the units. Enthalpic factors are viewed as specific interactions between interacting units at the surface of these units and will be argued to be related to the surface area of the units. It is believed that specific interactions are the basis of LCST behavior. In the third paper it will be argued that the manifestation of LCST behavior is predictable in terms of structural parameters such as the surface area and volume of the interacting units. Minor changes in structure which affect the surface area and volume of a PVME interacting unit will be shown to have proportional effects on the enthalpic and entropic parameters of the F–H–S analysis.

References and Notes

(1) Beaucage, G.; Stein, R. S.; Hashimoto, T.; Hasegawa, H. *Macromolecules* 1991, *24*, 3443–3448.

(2) Staverman, A. J. *Integration of Fundamental Polymer Science and Technology*; Kleintjens, L. A., Lemstra, P. J., Eds.; Elsevier Publishers: London, 1986; p 19. Koningsveld, R.; Kleintjens, L. A.; Leblans-Vinck, A. M. *J. Phys. Chem.* 1987, *91*, 6423–6428.

(3) Beckman, E. J.; Porter, R. S.; Koningsveld, R. *J. Phys. Chem.* 1987, *91*, 6429–6439. Also: paper to be published.

(4) Tompa, H. *Trans. Faraday Soc.* 1949, *45*, 1142.

(5) Koningsveld, R.; Staverman, A. J. *J. Polym. Sci., Polym. Phys. Eds.* 1968, *6*, 305, 325, 349.

(6) Koningsveld, R.; Staverman, A. J. *Kolloid Polym. Z.* 1968, *218*, 114.

(7) Koningsveld, R. *Adv. Colloid Interface Sci.* 1968, *2*, 151.

(8) Koningsveld, R. *Discuss. Faraday Soc.* 1970, *49*, 144.

(9) Staverman, A. J. *Recl. Trav. Chim. Pays–Bas* 1937, *56*, 885. Bondi, A. *J. Phys. Chem.* 1964, *68*, 441.

(10) Schweitzer, K. S.; Curro, J. G. *J. Chem. Phys.* 1989, *91* (8), 5059.

(11) Olabisi, O.; Robeson, L. M.; Shaw, M. T. *Polymer–Polymer Miscibility*; Academic Press: New York, 1979; Chapter 2.

(12) Karasz, F. E.; MacKnight, W. J. *Macromolecules* 1968, *1* (6), 537.

(13) Rubenstein, M.; Rubenstein, S. *Chem 3D, The Molecular Modeling System Version 2*; Cambridge Scientific Computing, Inc.: Cambridge, MA, 1989.

(14) Allinger, N. L. *J. Am. Chem. Soc.* 1977, *99* (25), 8127.

(15) Burkert, U.; Allinger, N. L. *Molecular Mechanics*; ACS Monograph Series 177; American Chemical Society: Washington, DC, 1982.